Dehydrogenation of 2,3-Butanediol to 3-Hydroxybutanone over CuZnAl Catalysts: Effect of Lithium Cation as Promoter

Boyu Zhang[1], Feng Zhou[2], Huixia Ma[2], Luning Chen[3], Ji Su[*,3], Xingzhou Yuan[1], Jian Zhang[*,1]

1 Liaoning Shihua University, Fushun 113001, PR CHINA
2 Dalian Research Institute of Petroleum and Petrochemicals, SINOPEC, Dalian 116000, PR CHINA
3 Materials Sciences Division, Lawrence Berkeley National Laboratory, Berkeley, California 94720, United States.

Corresponding author:
Prof. Jian Zhang:
Liaoning Shihua University
Fushun 113001, PR China
Tel: + 86-24-5686-3046
E-mail: zhangjian2011@lnpu.edu.cn

Dr. Ji Su:
Tel: +1-(510) 486-4829
E-mail: jisu@lbl.gov

Abstract: The dehydrogenation of 2,3-butanediol (BDO) to 3-hydroxybutanone (HBO) was studies over Li cation-doped CuZnAl catalysts. The catalyst samples were characterized by XRD, XPS, H_2-TPR and SEM techniques. The characterization results showing that doping with Li cation obviously modified the surface morphology of CuZnAl catalysts; decreased the reduction temperature of CuZnAl catalysts; and finally increased the amount of Cu active sites. The reaction results showing that, Li modified CuZnAl catalysts obviously enhanced the selectivity of the dehydrogenation of BDO to HBO by inhibiting the

dehydration of BDO. The Li(2%)-Cu(44%)- Zn(38%)-Al(16%) exhibited the highest activity for dehydrogenation of BDO, with the conversion rate of BDO is 72.4% and the selectivity of HBO is 95.9% at 260 °C. This catalyst shows excellent stability for more than 100 h without significant deactivation.

Keywords: 2,3-butanediol; 3-hydroxybutanone; Dehydrogenation reaction; Alkali metal modification; CuZnAl catalyst

1. Introduction

3-Hydroxybutanone (HBO), also known as acetoin, is naturally found in many foods, such as corn, grapes, apples and meat. It is a widely used flavoring spice with a pleasant creamy aroma, which is mainly added in cream, dairy, yogurt and strawberry flavored[1-2]. Furthermore, HBO has an important application in the wine industry, the product, containing 80% of HBO, plays a crucial role in liquor flavoring [3]. In addition, because of the typical aroma and beneficial effect on leaf fragrance, HBO is the main basis of the special aroma for the special flavor flue-cured tobacco. Efforts have been striven to expand apply in Europe, the United States and Japan. At present, there are three main industrial methods for HBO production: partial hydrogenation of 2,3-butanedione [4-5], selective oxidation of 2,3-butanediol[6-7] and chlorination and hydrolysis of butanone[8-9]. However, the weakness of these three methods are hard to be ignored, such as low yield, serious pollution and poor quality which is difficult to meet the flavoring requirements.

2,3-butanediol (BDO), also known as 2,3-bishydroxybutane, is an important chemical dye and liquid fuel, which is widely applied in the chemical, food, fuel and aerospace industries. Besides, it can also be dehydrogenated to acetoin by dehydrogenase [10-11]. The downstream

applications of BDO mainly include dehydration to prepare methyl ethyl ketone (MEK) and 2-methylpropanal. For example, Ai V. Tran et al. [12] investigated BDO catalytic dehydration to MEK, Zhang et al. [13] studied the efficient dehydration of BDO to MEK catalyzed by boric acid-modified HZSM-5, and Zheng et al. [14] investigated BDO dehydration to 2-methylpropanal catalyzed by Cu-based catalyst. In addition, BDO can as well be dehydrogenated to diacetyl, which is a high value-added food additive [15]. However, at present, there are still few studies on BDO dehydrogenation to prepare HBO, which is a far more promising platform chemical.

CuZnAl catalyst plays a crucial role in the chemical industry. It is widely used in alcohols dehydrogenation reaction to make correspond aldehydes and ketones [16-17], due to their well dispersion on the support, relatively low reaction temperature, high space velocity, large surface free energy and simple process. Liu et al. [18] studied cyclohexanol dehydrogenation to cyclohexanone based on CuZnAl catalyst, while Jung K D et al. [19] studied methanol catalytic dehydrogenation to acetic acid by CuZnAl catalyst. Although there are many studies on the alcohols dehydrogenation catalyzed by CuZnAl, the mechanism of catalytic reaction for dehydrogenation is still unclear [20]. F. Pepe et al [21] believed that Cu^0 is the only effective component in the dehydrogenation catalyst, the increase in Cu^+ content does little for activity enhancement. However, Herman et al. [22] proposed that the active site is the Cu^+ dissolved in zinc oxide by in-depth study on CuZnAl catalyst. Besides, Liu et al [23] investigated the catalytic performance of CuZnAl modified by Ga_2O_3 in methanol steam reforming reaction, showing that with Ga_2O_3 the reducibility of modified catalyst is improved. Tan et al [24] applied Mn modified CuZnAl in the synthesis of dimethyl ether (DME), they found that the catalyst has high activity and good stability, indicating that the addition of metal additives can modulate the catalytic performance of CuZnAl catalyst.

Herein, the promotion effect of Li cation on CuZnAl catalyst was in-depth studied in the reaction of selectively dehydrogenation of BDO to HBO. The CuZnAl catalyst was synthesized with co-precipitation method,[25] then different of Li content (1, 2, 4, 8wt. %) was doped by impregnation with different concentration of $LiNO_3$ solution. The characterization and reaction results showing that Li cation obviously decrease the reduction temperature of CuZnAl catalysts and increase the amount of Cu active sites. In the reaction of selectively dehydrogenation of BDO to HBO, the effect of Li cation significantly promotes the production of HBO and inhabit the competing reaction of DBO dehydration.

2. Experimental

2.1 Agents and instruments

$Cu(NO_3)_2{\cdot}3H_2O$, $Zn(NO_3)_2{\cdot}6H_2O$, $Al(NO_3)_2{\cdot}9H_2O$, $LiNO_3$, $Na_2(CO_3)_2$ and BDO were all analytically pure and purchased from Sinopharm Chemical Reagent Co., Ltd.

Magnetic stirrer (HJ-4, Jintan Ronghua Instrument Manufacturing Co., Ltd., Jiangsu Province); circulating water vacuum pump (SHZ-D, Gongyi City, China Instrument Co., Ltd.); electronic balance (WT-B1003, Hangzhou Wante Weighing Apparatus Co., Ltd.); desktop drying oven (101-1 EBS, Beijing Yongguangming Medical Instrument Co., Ltd.); constant temperature water bath (DF-101S, Gongyi, China Instrument Co., Ltd.); gas chromatograph (6890 plus, Agilent); Muffle furnace (SX2-4-10, Shenyang Industrial Electric Furnace Factory).

2.2 Preparation of catalysts

~~The CuZnAl catalyst was prepared by co-precipitation method. A typical preparation procedure is as follows:~~

The CuZnAl catalyst was prepared by co-precipitation method. A typical

preparation procedure is as follows:

$Cu(NO_3)_2$, $Zn(NO_3)_2$ and $Al(NO_3)_3$ were prepared and mixed to aqueous nitrate solution, the aqueous of the mixed metal nitrate solution with an atomic ratio of the metal components of 1:1:1 and then $Na_2(CO_3)_2$ aqueous solution (1mol/L) was added into the mixture as precipitant. Precipitation was carried out under 80 ° C. After the precipitation, the mother liquor was aged for 6 h, and filtered and washed with deionized water, then dried at 100 °C for 8 h, and calcined at 500 ° C for 4 h, the CuZnAl catalyst was obtained. The molar ratio of CuZnAl catalyst is 4.5:4.5:1.

The Li modified CuZnAl catalyst was prepared by the impregnation method. The specific method is as follows: a certain concentration of $LiNO_3$ solution was prepared, and then added dropwise to the CuZnAl catalyst with stirring at room temperature. After stirring for 12 h, the sample was dried at 100 °C for 8 h, and then calcined in air at 500 °C for 4 h. Finally, a Li-modified CuZnAl catalyst was obtained, which was denoted as Li-CuZnAl. The element ratios of different modified Li content were analyzed and shown in table 1.

Table 1. Chemical compositions of different Li content catalysts

Sample	CuO(wt%)	ZnO(wt%)	Al_2O_3(wt%)	Li_2O(wt%)
1 wt.% of CuZnAl	42.4	43.6	13	1
2 wt.% of CuZnAl	42.6	42.9	12.5	2
4 wt.% of CuZnAl	41.3	43	11.7	4
8 wt.% of CuZnAl	39.7	40.7	11.6	8

2.3 Catalyst characterization

The crystal structure of the sample was analyzed by XRD-7000 X-ray

diffraction (XRD) from Shimadzu Corporation of Japan; XPS characterization was performed using a PHI 5000 Versa Probe electron spectrometer from UIVAC-PHI Corporation of Japan. The specific surface area of samples was measured by Microscales 2010 physical adsorption instrument from American Instruments and scanning electron microscopy (SEM) images were recorded on a JEOL JSM-6380-LA high resolution transmission electron microscope. The surface morphology of samples was observed on a Japanese Hitachi SU8010 field emission electron scanning microscope. The samples were characterized by H_2-TPR using a Conta TPD/TDR-Pulsar fully automated dynamic chemisorption analyzer.

2.4 Catalyst performance

The performance of the catalyst for the dehydrogenation of BDO to HBO was evaluated in a continuously flowing fixed bed reactor. The reactor was a stainless steel microreactor with an internal diameter of 10 mm. 2 g of the catalyst (20-40 mesh) was weighed and packed into the constant temperature zone of the reactor, and the upper and lower sections of the catalyst bed were packed with quartz sand (20-40 mesh). Reduction needed to be carried out first. The procedure is as follows: The reaction tube was heated from room temperature to 260 °C at a rate of 5 °C/min and kept for 4 h under a mixed atmosphere of hydrogen (10%) and nitrogen (90%). After the reduction finished, it was cooled to the reaction temperature with N_2. And then, BDO was fed into the reactor by a constant current pump, and the sample was collected after being stabilized for 3 hours and vent at each testing temperature point. The product was analyzed by Agilent 7890A gas chromatography with capillary column and hydrogen flame detector (FID). The oven program: 60 °C for 6 minutes, rise to 220 °C at a rate of 10 °C/min and keep for 10 minutes. The performance of the catalyst was characterized by the conversion of 2,3-butanediol, the selectivity and yield of 3-hydroxybutanone. Reaction condition: atmospheric, temperature=250~280

°C, LHSV=0.05~0.3 h^{-1}. The 2,3-butanediol conversion and selectivity are calculated by chromatographic analysis. The formula of BDO's conversion is:

$$\alpha\%=1-\frac{C}{C_0}\times 100\%$$

C0 is the concentration of 2,3-butanediol in the raw material, C is the concentration of 2,3-butanediol after the reaction in the product.

The formula of HBO's selectivity is:

$$\beta\%=\frac{C_a}{(\frac{C_0-C}{M_{BDO}})\times M_{HBO}}\times 100\%$$

C_a is the concentration of 3-hydroxybutanone in the product, M_{BDO} is the molar mass of the 2,3-butanediol, M_{HBO} is the molar mass of the 3-hydroxybutanone.

The formula of HBO's yield is:

$$\gamma\%=\alpha\%\times\beta\%$$

3. Results and discussion

3.1. Catalyst Characterization

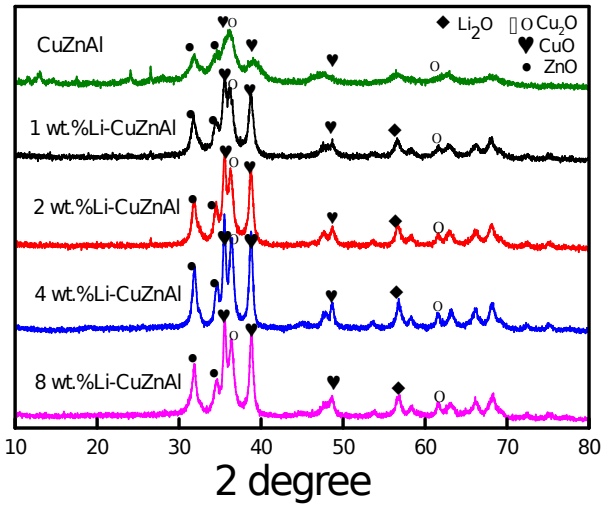

Fig.1 XRD patterns of CuZnAl and Li-CuZnAl catalysts

The XRD patterns of as-prepared Li-CuZnAl catalysts, which calcined at 500 °C in air after the promotion with different Li contents, are shown in Figure 1. No obvious diffraction peaks were observed in the XRD patterns of the supports Al_2O_3 before and after Li promotion, revealing that tuning Li contents did not influence the amorphous phases of the Al2O3 supports. In the case of the Cu and Zn contents, the XRD patterns were very different from that of the Al_2O_3 supports. Specifically, the height and area of the diffraction peaks (2θ = 35.5°, 38.7 °, 48.8 °) of the CuO phase [26], and the peaks (2θ =36.52 ° and 61.46 °) of Cu_2O phase [27], as well as the diffraction peaks (2θ =22.8 °, 34.3 °, 36.1 °) of ZnO phase [26], were obviously increased after the Li promotion. These results indicate that Li promotion distinctly change the crystallinity and orientation of Cu and Zn contents. More interestingly, the half-peak width of these peaks was significantly decreased, which means that the size of CuO, Cu_2O and ZnO crystalline were reduced by the Li modification. A similar effect was also found in the previous study [28]. And this crystalline size reduction will increase the surface area and favor the catalytic reaction. On the other hand, Figure 1 also showed that the enlargement of the peaks of CuO phase (such as the peak 2θ = 38.7 °) are more remarkable than the Cu_2O phase, which means the ratio of CuO to Cu_2O may be increased by Li modification. A peak located around 66-67 ° was generated by Li promotion. According to the literature this peak should be attributed to spinel-type $CuAl_2O_4$ nanocrystalline [29,30], which was proved could enhance the long-term stability by increasing the resistance to sintering of the catalyst and also further decrease the size of Cu species. The characteristic diffraction peak position of Li_2O is 2θ = 56.6 ° and 33.9 °, the characteristic diffraction peak of Li_2O overlaps because it is very close to the characteristic diffraction peak of ZnO. With the increase of Li content,

the diffraction peak intensity of Li2O was the strongest at 4 wt. % and weakest at 2 wt. %, This proved that Li_2O in 2 wt. % catalyst had the best dispersion. This is consistent with our experimental results. In the CuZnAl catalyst, we also observed a wide peak near 2θ =56.6°, because of the characteristic diffraction peaks of CuO and ZnO in this region, we believed that CuO/ZnO co-solution was formed in the co-precipitation process.

Finally, these findings clearly revealed that the effects of Li promotion/modification including: 1) increased the crystallinity and decrease the size of CuO, Cu_2O and ZnO crystalline; 2) increased the ratio of CuO to Cu_2O; 3) generated a spinel-type $CuAl_2O_4$ nanocrystalline. And more, the Li contents also influence the promotion performance. Excessive Li_2O will decrease crystallinity and cover the surface of Cu species, for example, when the introduction amount of Li is 8 wt. %, the peak intensity of Cu_2O is significantly reduced.

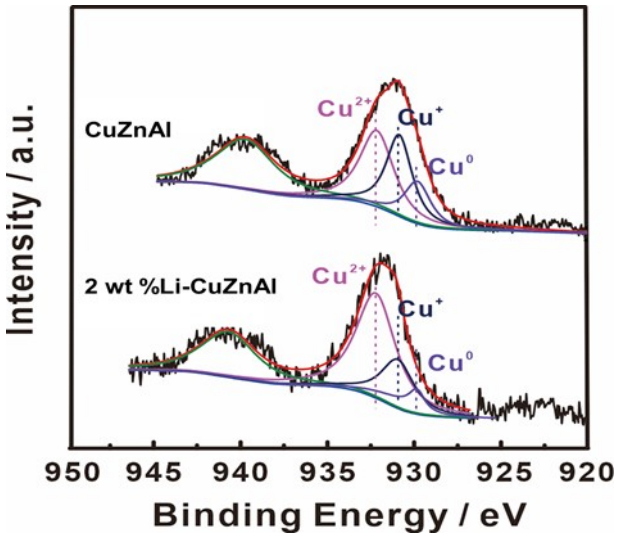

Fig. 2 XPS spectra of CuZnAl and 2 wt. % of Li-CuZnAl

Figure 2 shows XPS spectrum of CuZnAl catalyst samples before and after Li (2 wt. %) modification. The binding energy peaks around 930 to 935 eV corresponded to Cu^0 and Cu^+, and Cu^{2+} species [31,32]. As shown in Figure 2, the peak shifted to higher binding energy which indicate more CuO was

generated on the surface of CuZnAl catalyst. And more, the ratio of CuO/Cu_2O on the surface was obviously increased which is matched with the XRD results in Figure 1. According to the results of XRD in Figure1, Li promotion obviously modified the distribution of the Cu species in the CuZnAl catalyst due to the strong electron donation effect of Li[33].

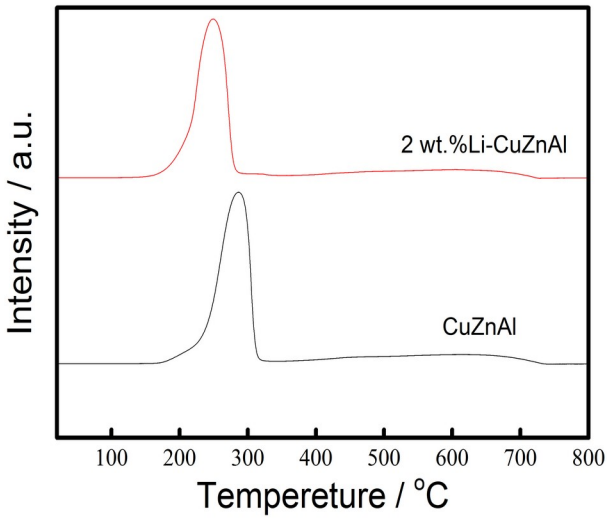

Fig. 3 H_2-TPR diagram of CuZnAl and 2 wt. % of Li-CuZnAl

The reduction behaviors of the catalyst samples of CuZnAl and Li-CuZnAl (2 wt. %) were studied by H_2-TPR, and the results were presented in Figure 3. As displayed in Figure 3, the H_2-TPR profile of both of CuZnAl catalyst samples before and after 2 wt % Li modification have two groups reduction peaks located at around 150-350 and 400-700 °C, which corresponded to the reduction of CuO/Cu_2O and $CuAlO_X$, respectively [34]. Firstly, as shown in Figure 3, most of Cu species in our co-precipitation method synthesized samples are CuO/Cu_2O which could be reduced to Cu metal below 350 °C by H_2 [35]. Secondly, the two hydrogen-consuming peaks are asymmetrical and trailing, suggesting that the reducible oxides are polymorphic, and the reduction is carried out species by species [36]. Thirdly, Li modification obviously further decrease the reduction temperature. The reduction mechanism for CuO and Cu_2O by H_2 was

investigated in detail [37], and results showing that the apparent activation energy for the reduction of CuO is about 14.5 kcal/mol, while the value is 27.4 kcal/mol for Cu_2O. Therefore, the reduction of CuO is easier than the reduction of Cu_2O. Combining our XRD results in Figure 1 which showing the Li modification increase the ratio of CuO/Cu_2O, the conclusion is that the Li promotion/modification enhance the formation of CuO, which is more easily to be reduced. The peak area in Figure 3 correspond to H_2 consumption, a larger peak area of Li modified CuZnAl catalyst indicate more CuO was reduced during the H_2 treatment, due to the different H_2 consumption rate of CuO and Cu_2O.

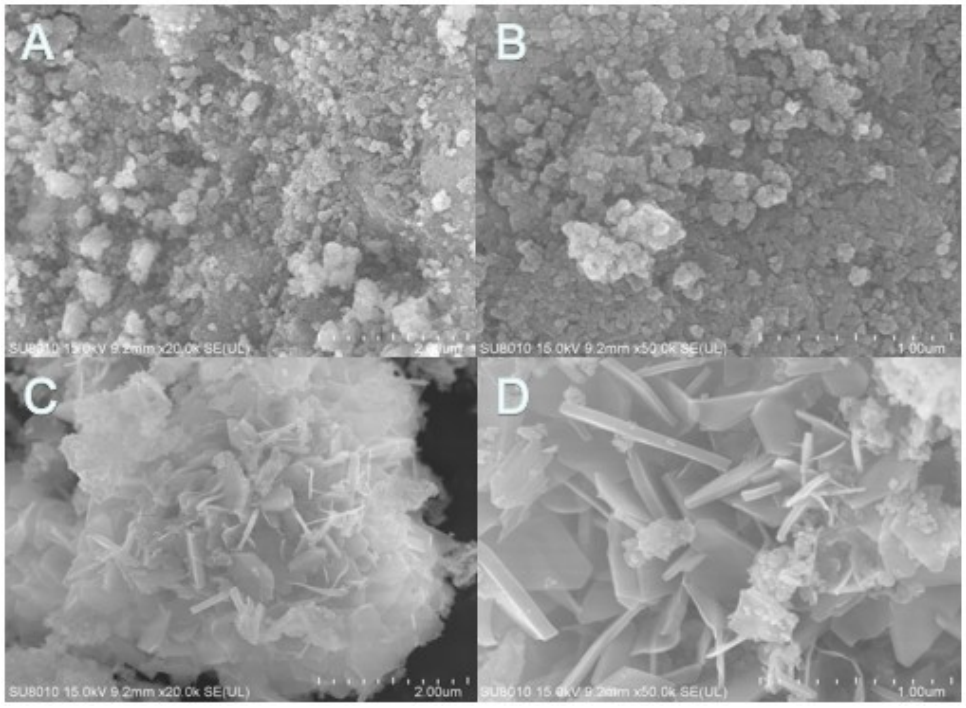

Fig. 4 SEM images of CuZnAl (A, B) and 2 wt. % of Li-CuZnAl (C, D)

The SEM images of CuZnAl (A, B) and 2 wt. % of Li-CuZnAl (C, D) are shown in Figure 4. It is showing that the Li promotion/modification significantly re-constructed the surface of CuZnAl catalyst. The surface of the fresh CuZnAl catalyst which prepared by co-precipitation method exhibits a massive structure, and particles aggregate to each other by the

interaction of hydrogen bonds and van der Waals forces [38]. After the Li modification, a large amount of spinel structure crystals was formed, which obviously change the morphology and increase the crystallinity of CuZnAl catalyst. That results are coincident with the XRD results in Figure 1.

Table 2. Physico-chemical parameters of the CuZnAl and 2 wt. % of Li-CuZnAl catalysts

Samples	Pore Diameter(nm)	Pore Volume(cm^3/g)	Surface Area(m^2/g)
CuZnAl	0.755	0.247	217.204
2 wt. % of Li-CuZnAl	0.631	0.281	204.969

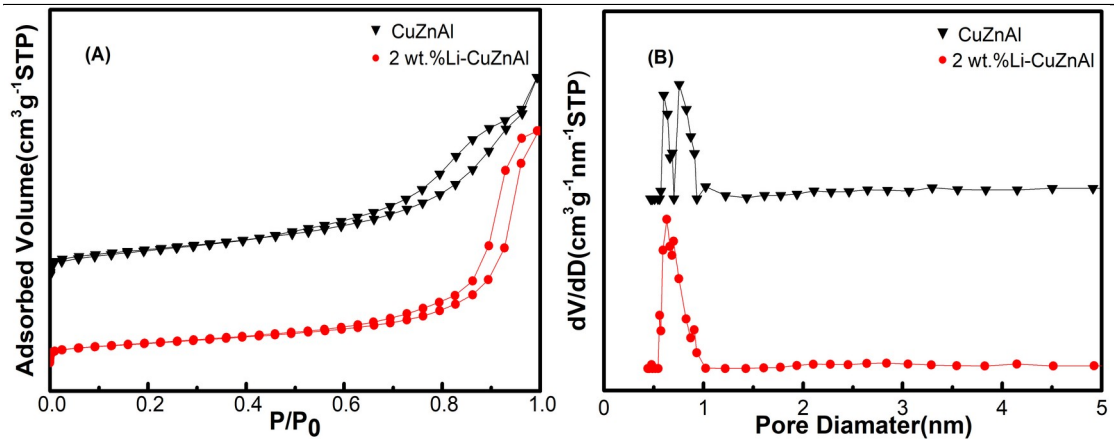

Fig. 5 N_2 adsorption-desorption isotherms of the CuZnAl and 2 wt. % of Li-CuZnAl (A) and the BJH of the CuZnAl and 2 wt. % of Li-CuZnAl (B)

The textural properties and the chemical compositions of the catalysts of the CuZnAl and 2 wt. % of Li-CuZnAl are listed in Table 2. Clearly decrease in the specific surface areas of the catalysts could be observed after Li modified. The catalyst CuZnAl shows higher specific surface areas of ca. 217.204 m^2/g, while the value for 2 wt. % of Li-CuZnAl is decreased to 204.969 m^2/g, indicating that the Li modified in the catalyst could adversely impact the structure of the supports. The N_2 adsorption-desorption results show that all the catalysts display the hysteresis loop with type IV, confirming the presence of the mesoporous structures in the catalysts. Fig. 5B illustrates after Li was modified, the pore distribution of the catalyst became relatively concentrated which the Mean pore-size decreased from 0.755 nm to 0.631 nm. The CuZnAl catalyst shows the highest peak intensity at about 0.6 nm and 0.75 nm and the 2 wt. % of Li-CuZnAl catalyst only shows one peak at about 0.6nm, suggesting that Li modified in the CuZnAl catalyst would destroy the porous structure. The 2 wt. % of Li-CuZnAl exhibits lower pore diameter and surface

area illustrates Li_2O is attached to the catalyst surface, blocking part of the channel, so that the specific surface area of the catalyst decreases. The new composition of $CuAl_2O_4$ enhance the interaction between Cu, Zn and Al would also reduce the pore diameter and specific surface area.

The catalytic performance of the Li modified catalyst samples for the dehydrogenation of BDO to HBO was evaluated in a continuously flowing fixed bed reactor. As shown in Figure 6, under the reaction temperature of 260 °C, both the conversion of BDO and the selectivity of HBO showing a volcanic curve with the 2 wt. % of Li-CuZnAl shows the highest BDO conversion of 72.4%, HBO selectivity of 95.9%, and the yield of 69.4%. According to characterization results, Li modification create a spinel structure of $CuZnAlO_x$ crystals, which have a lower reduction temperature in presence of H_2, which means after Li modification more Cu^0 species were generated and they are crucial for the dehydrogenation reaction. On the other hand, the excess amount of Li can cover the Cu^+ active centers on the catalyst surface and hinder the reduction of Cu^{2+}. However, the insufficient amount of Li would result in deficient electron effect, and then decreasing the number of Cu^+ active centers.

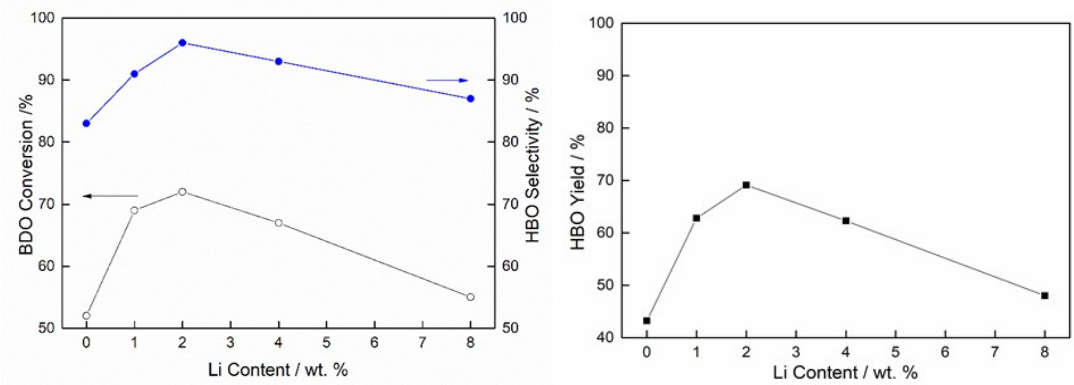

Fig.6 Dehydrogenation of BDO catalyzed by CuZnAl and Li-CuZnAl catalyst with different Li contents

Reaction condition: 0.1 MPa, 260 °C, LHSV=0.1 h^{-1}

Fig. 7 showed the temperature dependence of the two catalysts before and after 2 wt % of Li modification. It indicates that under the same conditions, the 2 wt. % of Li-CuZnAl shows higher catalytic performance for dehydrogenation of BDO than that of CuZnAl. According to the results of XPS and H_2-TPR, the reduction temperature of the catalyst is lowered after the addition of Li since the electron effect of Li increases the number of Cu

active centers, thereby improving the performance of the catalyst. The activity of the two catalysts shows that the conversion of BDO is increased with the temperature rising, while the selectivity of HBO is decreased. The optimum reaction temperature is 260 °C, and under such condition, the conversion of BDO is 72.4%, the selectivity of HBO is 95.9%, and the yield is 69.4%.

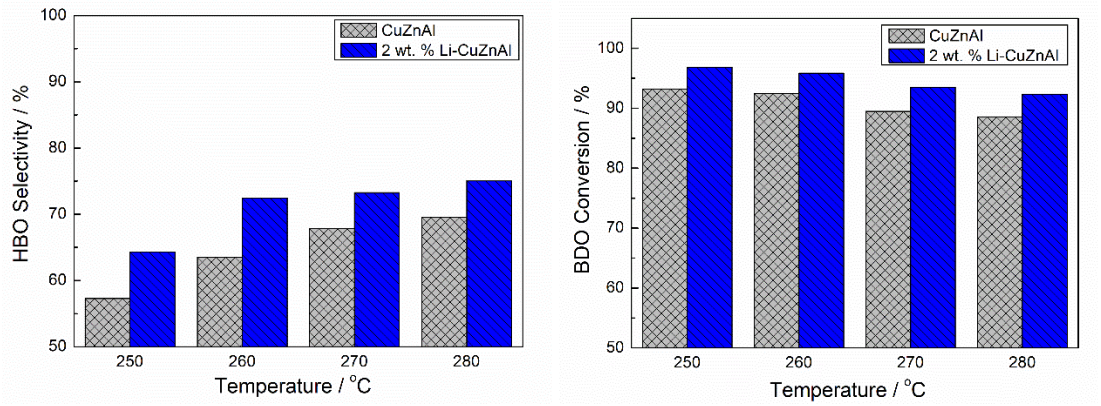

Fig.7 Dehydrogenation of BDO catalyzed by CuZnAl and 2 wt. % of Li-CuZnAl

Reaction condition: 0.1 MPa, 250~280 °C, LHSV=0.1 h^{-1}

The effect of space velocity on the dehydrogenation performance of BDO catalyzed by 2 wt. % of Li-CuZnAl was studied, as shown in Fig. 8. As the space velocity increased from 0.05 h^{-1} to 0.3 h^{-1}, and the conversion of BDO increased from 69.8% to 72.4%, and then decreased to 62.7%, while HBO selectivity increased from 92.3% to 97.1%. The maximum product yield appeared at 0.1 h^{-1}, which was 69.4%.

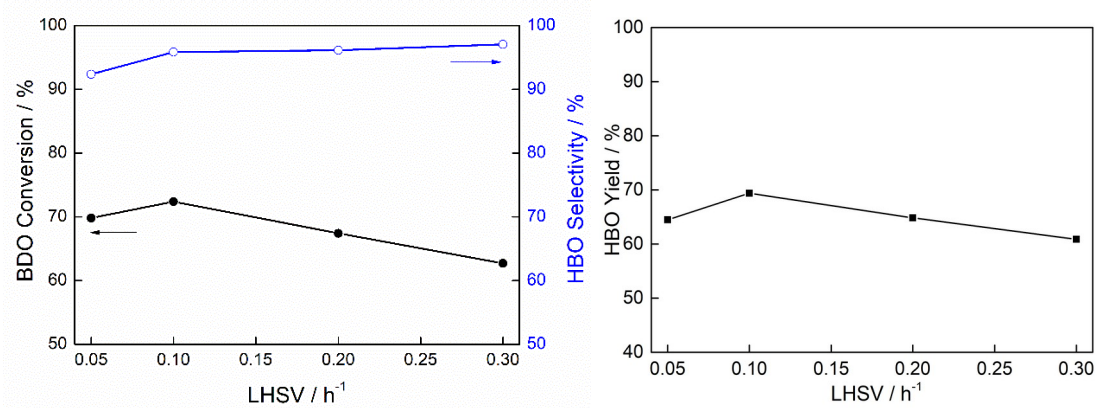

Fig. 8 Effect of space velocity on BDO dehydrogenation catalyzed by 2 wt. % of Li-CuZnAl

Reaction condition: 0.1 MPa, 260 °C, LHSV=0.05~0.3 h^{-1}

Most of the industrial chemical reaction are conducted at medium to high temperatures. Catalysts that are used to make these processes feasible have to be not only active, but also stable under reaction conditions for extended periods of time. The study of catalyst stability is crucial. Fig. 9 shows the stability of the 2 wt. % of Li-CuZnAl in the BDO dehydrogenation which was conducted at 260 °C and 0.1 h^{-1}(LHSV). It indicates that 2 wt. % of Li-CuZnAl exerts excellent stability in BDO dehydrogenation to HBO. During the 100 h of operation, BDO conversion is maintained at about 72%, HBO selectivity is around 96%, and the yield is around 70%.

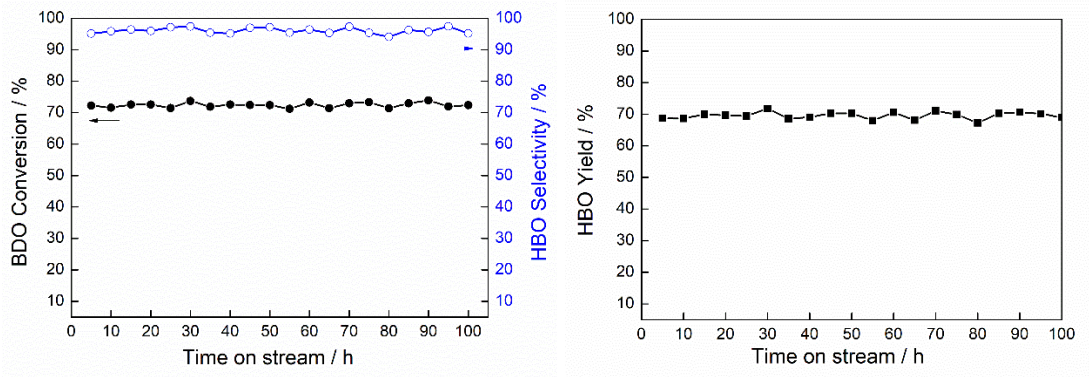

Fig. 9 Stability study on 2 wt. % of Li-CuZnAl

Reaction condition: 0.1 MPa, 260 °C, LHSV=0.1 h^{-1}

According to figure 9, we found that the selectivity and conversion rate of BDO did not change significantly after a long reaction. XRD characterization of 2 wt. % Li-CuZnAl was carried out after 100 h reaction. The characteristic diffraction peak of CuO disappeared after the reaction. It has been reported that the active site of alcohol dehydrogenation reaction is Cu^0/Cu^+ [39], this is consistent with the XRD pattern after the reaction. The diffraction peaks of ZnO. Li_2O and Cu_2O in the catalyst did not change position compared with those before the reaction, indicating that the physical structure of the catalyst was stable in the reaction process, which should be the reason for the long-term stability of the catalyst. After the reaction, there was a diffraction peak of carbon deposition in the catalyst, which indicated that carbon deposition would be generated by partial sintering after a long reaction in the catalyst, but this phenomenon had no obvious effect on the catalytic activity of the catalyst.

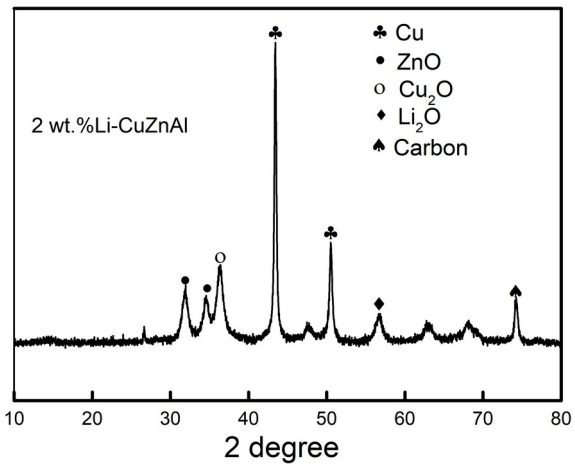

Fig.10 XRD patterns of 2 wt. % Li-CuZnAl after 100h reaction

3 Conclusion

The promotion effect of Li cation on CuZnAl catalyst was studied in the dehydrogenation of 2,3-butanediol to 3-hydroxybutanone. Importantly, the characterization results showing that Li-CuZnAl can decrease the reduction temperature of CuO and increase the specific surface area, and the electron donating effect of Li can increase the charge density of the catalyst surface, thereby improving the performance. The excessive amount of Li will cover the surface active sites and reduce the performance. Therefore, 2 wt. % of Li-CuZnAl catalyst shows the best performance. Under the conditions of 260 ^{o}C, 0.1 $h^{-1}$and 0.1MPa, the conversion of BDO is 72.4%, the selectivity of HBO is 95.9%, the yield of product is 69.4%. Meanwhile, the catalyst presents excellent stability, and can be operated continuously for at least 100 h without significant change in properties.

Conflict of interest

The authors declare that they have no conflict of interest.

References

1. Molinnus D, Muschallik L, Gonzalez LO, Bongaerts J, Wagner T, Selmer T, Siegert P, Keusgen M, SchÖning MJ (2018) Development and characterization of a field-effect biosensor for the detection of acetoin. Biosens Bioelectron

115:1-6. https://doi.org/10.1016/j.bios.2018.05.023

2. Xiao Z, Lu J (2014) Generation of acetoin and its derivatives in foods. J SCI Food Agr 62:6487-6497. https://doi.org/10.1021/jf5013902

3. Toda F, Tanaka K, Tange H (1989) Cheminform abstract: new reduction method of α-diketones, oxo amides, and quinones with Zn-EtOH in the presence of a salt. Cheminform, 20(49), 1555-1556. https://doi.org/10.1002/chin.198949081

4. Faveri DD, Torre P, Molinari F, Perego P, Converti A (2003) Carbon material balances and bioenergetics of 2,3-butanediol bio-oxidation by acetobacter hansenii. Enzyme Microb Tech 33(5):708-719. https://doi.org/10.1016/S0141-0229(03)00218-7

5. Romano A, Gandolfi R, Nitti P (2002) Acetic acid bacteria as enantioselective biocatalysts. J Mol Catal B-Enzym 17(6):235-240. https://doi.org/10.1016/S1381-1177(02)00013-9

6. Jónsdóttir R, ólafsdóttir G, Chanie E , Haugen JE (2008) Volatile compounds suitable for rapid detection as quality indicators of cold smoked salmon (salmo salar). Food Chem 19(1):184-195. https://doi.org/10.1016/j.foodchem.2007.12.006

7. David C, Robacker CR, He X (2004) Volatiles production and attractiveness to the mexican fruit fly ofenterobacter agglomeransisolated from apple maggot and mexican fruit flies. J Chem Ecol 30(7):1329-1347. https://doi.org/10.1023/b:joec.0000037743.98703.43

8. Xiao Z, Xu P (2007) Acetoin metabolism in bacteria. Crit rev Microbiol 33(2):127-140.https://doi.org/10.1080/10408410701364604

9. Gu Y, Duan X, Yang L, Guo L (2017) Direct C-H cyanoalkylation of heteroaromatic n-oxides and quinones via C-C bond cleavage of cyclobutanone oximes. Org Lett 19(21):5908-5911. https://doi.org/10.1021/acs.orglett.7b02902

10. Duan H, Sun D, Yamada Y, Sato S (2014) Dehydration of 2,3-butanediol into 3-buten-2-ol catalyzed by ZrO_2. Catal Commun 48:1-4. https://doi.org/10.1016/j.catcom.2014.01.018

11. Zhang L, Singh R, Sivakumar D, Guo Z, Li J, Chen F, He Y, Guan X, Kang YC, Lee J-K (2017) Artificial synthetic pathway for acetoin, 2,3-butanediol, and 2-butanol production from ethanol using cell free multi-enzyme catalysis. Green Chem 10:2-42. https://doi.org/10.1039/C7GC02898A

12. Song D (2016) Kinetic model development for dehydration of 2,3-butanediol to 1,3-butadiene and methyl ethyl ketone over an amorphous calcium phosphate catalyst. Ind Eng Chem Res 14:2-25.

https://doi.org/10.1021/acs.iecr.6b02930

13. Zhang W, Yu D, Ji X, Huang H (2012) Efficient dehydration of bio-based 2,3-butanediol to butanone over boric acid modified HZSM-5 zeolites. Green Chemistry, 14(12):3441-3450. https://doi.org/10.1039/c2gc36324k

14. Zheng Q, Xu J, Liu B, Hohn K (2018) Mechanistic study of the catalytic conversion of 2,3-butanediol to butenes. J Catal 360:221-239. https://doi.org/10.1016/j.jcat.2018.01.034

15. Yen H-W, Li F, Wong CL (2014) The PH effects on the distribution of 1,3-propanediol and 2,3-butanediol produced simultaneously by using an isolated indigenous klebsiella sp.Ana-WS5. Bioproc Biosyst Eng 37(3):425-431. https://doi.org/10.1007/s00449-013-1008-1

16. Sato S, Takahashi R, Fukuda H, Lnui K (2007) Dehydrogenation of 1,3-butanediol over Cu-based catalyst. J Mol Catal A 272:164-168. https://doi.org/10.1016/j.molcata.2007.03.034

17. Zhang Q, Wu Z, Xu L (1998) High-Pressure hydrogenolysis of diethyl maleate on Cu-Zn-Al-O catalysts. Ind Eng Chem Res 37(9):3525-3532. https://doi.org/10.1021/ie980178i

18. Liu X, Wang L, Yan K, Zhang L, Xie X (2009) The study on the dehydrogenation ofcyclohexanol over complex oxides derived from CuZnAl hydrotalcite-like. Chemical Research & Application 21(9):1250-1254. https://doi.org/10.1002/chir.20634

19.Jung K-D, Joo O-S. Preparation of $Cu/ZnO/M_2O_3$ (M = Al, Cr) Catalyst to stabilize Cu/ZnO catalyst in methanol dehydrogenation. Catal Lett, 2002, 84(1): 24-25. https://doi.org/10.1023/A:1021060130786

20. Popova M, Dimitrov M, Santo VD, Ravasio N, Scotti N (2012) Dehydrogenation of cyclohexanol on copper containing catalysts:the role of the support and the preparation method. Catal Commun 17:150-153. https://doi.org/10.1016/j.catcom.2011.10.021

21. Pepe F, Angeletti C, Rossi SD, Jacono ML (1985) Catalytic behavior and surface chemistry of copper/alumina catalysts for isopropanol decomposition. J Catal 91(1):69-77. https://doi.org/10.1016/0021-9517(85)90289-1

22. Herman R, Klier K, Simmons G, Finn B, Bulko J, Kobylinski T (1979) Catalytic synthesis of methanol from carbon monoxide/hydrogen. phase composition, electronic properties,and activities of the copper/zinc $Oxide/M_2O_3$ catalysts. Cheminform 10(25):456-460. https://doi.org/10.1002/chin.197925142

23. Liu X, Toyir J, Piscina PRDL, Homs N (2017) Hydrogen production from

methanol steam reforming over Al_2O_3-and ZrO_2-modified. Int J Hydrogen Energ 42(19):13704-13711. https://doi.org/10.1016/j.ijhydene.2016.12.133

24. Tan Y, Xie H, Cui H, Han Y, Zhong B (2005) Modification of Cu-based methanol synthesis catalyst for dimethyl ether synthesis from syngas in slurry phase. Catal Today 104(1):25-29. https://doi.org/10.1016/j.cattod.2005.03.033

25. Park N-J (1996) Texture in CuZnAl shape memory alloys. Met Mater Int 2(3):159-168.
https://doi.org/10.1007/BF03026090

26. Velu S, Suzuki K, Okazaki M, Kapoor MP, Osaki T, Ohashi F (2000) Oxidative steam reforming of methanol over CuZnAl(Zr)-oxide catalysts for the selective production of hydrogen for fuel cells: catalyst characterization and performance evaluation. J Catal 194(2):373-384. https://doi.org/10.1006/jcat.2000.2940

27. Huang W, Yu L, Li W, Ma Z (2010) Synthesis of methanol and ethanol over CuZnAl slurry catalyst prepared by complete liquid-phase technology. Front Chem Eng China 4(4):472-475. https://doi.org/10.1007/s11705-010-0525-6

28. Choi SM, Kang YJ, kim SW (2018) Effect of γ-alumina nanorods on CO hydrogenation to higher alcohols over lithium-promoted CuZn-based catalysts. Appl Catal A-Gen 549:188-196. https://doi.org/10.1016/j.apcata.2017.10.001

29. Salavati-Niasari M, Davar F, Farhadi M (2009) Synthesis and characterization of spinel-type $CuAl_2O_4$ nanocrystalline by modified sol–gel method. J Sol-Gel Sci Technol 51(1):48-52. https://doi.org/10.1007/s10971-009-1940-3

30. Chinchen GC, Denny PJ, jennings JR, Spencer MS, Waugh KC (1988) Synthesis of Methanol: Part 1. Catalysts and Kinetics. Appl Catal 36(1-2):1-65. https://doi.org/10.1016/S0166-9834(00)80103-7

31. Gao Z, Li S, Tian H, Dong W, Liu Y, Jia L, Huang W (2017) Synthesis of ethanol from syngas over CuZnAl catalysts with different Cu/Zn/Al molar ratios in polyethylene glycol 600 medium. React Kinet Mech Cat 122(2):1-11. https://doi.org/10.1007/s11144-017-1270-3

32. Gao Z, Huang W, Wang J, Yin L, Xie K (2008) Studies on the structure and catalyticperformance of Cu-Zn-Al catalyst prepared by liquid-phase preparation technology under different heat treatment atmosphere. J Nat Gas Chem 66(3):295-300. https://doi.org/10.1016/S1003-9953(09)60131-6

33. Liu Y, Lei J, Deng X, Huang W, Vinokurov VA (2018) Promotional influence of hydroxyl complexing agent on ethanol synthesis from syngas over CuZnAl catalysts without other metal promoters. Catal Lett 148(11) 3477-3485. https://doi.org/10.1007/s10562-018-2545-7

34. Li X, Zhang J, Zhang M, Zhang W, Zhang M, Xie H, Wu Y, Tan Y, The Support Effects on the Direct Conversion of Syngas to Higher Alcohol Synthesis over Copper-Based Catalysts, Catalysts 2019, 9(2), 199; https://doi.org/10.3390/catal9020199

35. Gao P, Li F, Zhan H, Zhao N, Xiao F, Wei W, Zhong L, Wang H, Sun Y (2013) Influence of Zr on the performance of Cu/Zn/Al/Zr catalysts via hydrotalcite-like precursors for CO_2 hydrogenation to methanol. J Catal 298:51-56. https://doi.org/10.1016/j.jcat.2012.10.030

36. Kühl S, Tarasov A, Zander S, Kasatkin I, Behrens M (2014) Cu-based catalyst resulting from a Cu, Zn, Al, hydrotalcite-like compound: A microstructural, thermoanalytical, and in-situ XAS study. Chem-Eur J 20(13):3782-3792. https://doi.org/10.1002/chem.201302599

37. Gao J, Thomas DA, Sohn CH, Beauchamp JL (2013) Biomimetic reagents for the selective free radical and acid–base chemistry of glycans: application to glycan structure determination by mass spectrometry. J Am Chem Soc 135(29):10684-10692. https://doi.org/10.1021/ja402810t

38. Wang C, Wang Y–, Liu W, Yin H, Yuan Z, Wang Q, Xie H, Cheng R (2012) Naturalfibrous nanoclay reinforced soy polyol-based polyurethane. Mater Lett 78:85-87. https://doi.org/10.1016/j.matlet.2012.03.067

39. Shishido T, Yamamoto M, Li D, Tian Y (2006) Water-gas shift reaction over Cu/ZnO and Cu/ZnO/Al_2O_3 catalysts prepared by homogeneous precipitation. Appl Catal A-Gen, 303(1), 62-71. https://doi.org/ 10.1016/j.apcata.2006.01.031